Inflammation, Vol. 37, No. 2, April 2014 (© 2013)
DOI: 10.1007/s10753-013-9741-9

Emodin-6-*O*-β-D–glucoside Inhibits High-Glucose-Induced Vascular Inflammation

Wonhwa Lee,[1,2] Sae-Kwang Ku,[3] Doohyun Lee,[1] Taeho Lee,[1] and Jong-Sup Bae[1,4]

Abstract—Emodin-6-*O*-β-D-glucoside (EG), a new active compound from *Reynoutria japonica*, has recently been shown to exert potent anti-inflammatory and barrier protective effects in human umbilical vein endothelial cells (HUVECs) and in mice. Vascular inflammatory process has been suggested to play a key role in initiation and progression of atherosclerosis, a major complication of diabetes mellitus. Thus, we attempted to determine whether EG can suppress the vascular inflammatory process induced by high glucose (HG) in HUVECs and mice. Data showed that HG induced markedly increased vascular permeability, monocyte adhesion, expressions of CAMs, formation of ROS, and activation of NF-κB. Remarkably, all of the above-mentioned vascular inflammatory effects of HG were attenuated by pretreatment with EG. Vascular inflammatory responses induced by HG are critical events underlying development of various diabetic complications; therefore, our results suggest that EG may have significant therapeutic benefits against diabetic complications and atherosclerosis.

KEY WORDS: emodin-6-*O*-β-D-glucoside; high glucose; HUVEC; inflammation; atherosclerosis.

INTRODUCTION

Diabetes is a group of chronic diseases characterized by hyperglycemia; hyperglycemia is believed to be an important regulator of vascular lesion development [1]. Accelerated small- and large-vessel disease is the leading cause of morbidity and mortality in patients with diabetes mellitus [2]. Hyperglycemia-induced endothelial dysfunctions, along with hypercoagulable potential of diabetes mellitus, accelerate the process of atherothrombotic complications [1, 3]. A vast array of lifestyle and pharmaceutical interventions aimed at prevention and control of hyperglycemia is used in administration of modern medical care [3]. In addition to ensuring adequate delivery of glucose to tissues of the body, treatment of diabetes attempts to decrease the likelihood that tissues of the body are harmed by hyperglycemia [3].

Two key early events in the pathogenesis of atherosclerosis are adhesion of monocytes to the endothelium followed by transmigration into the subendothelial space and enhanced vascular cellular permeability [4, 5]. Increased leukocyte–endothelial interactions with monocytes from *in vivo* and *in vitro* diabetes models have been demonstrated [4, 6]. Of particular importance, the hyperglycemia-/high-glucose (HG)-induced augmentation of leukocyte adhesion to the endothelium through the upregulation of cell surface expression of adhesion molecules and transendothelial migration (TEM) has been reported to be dependent on NF-κB activation [7, 8]. In addition, endothelial cell permeability is impaired in diabetes mellitus and may be increased by high concentrations of extracellular glucose [5]. Leakage of serum proteins, particularly albumin, through the endothelium is observed in retinal vessels early in diabetes mellitus [5, 9]. Similarly, an increase in endothelial permeability has been implicated in early diabetic nephropathy [10]. Increased

Wonhwa Lee and Sae-Kwang Ku contributed equally to this work.

Electronic supplementary material The online version of this article (doi:10.1007/s10753-013-9741-9) contains supplementary material, which is available to authorized users.

[1] College of Pharmacy, CMRI, Research Institute of Pharmaceutical Sciences, Kyungpook National University, 80 Dahak-ro, Buk-gu, Daegu 702-701, Republic of Korea
[2] Department of Biochemistry and Cell Biology, School of Medicine, Kyungpook National University, Daegu 702-701, Republic of Korea
[3] Department of Anatomy and Histology, College of Oriental Medicine, Daegu Haany University, Gyeongsan 712-715, Republic of Korea
[4] To whom correspondence should be addressed at College of Pharmacy, CMRI, Research Institute of Pharmaceutical Sciences, Kyungpook National University, 80 Dahak-ro, Buk-gu, Daegu 702-701, Republic of Korea. E-mail: baejs@knu.ac.kr

endothelial cell permeability in larger vessels leads to development of interstitial edema and may result in enhancement of cell proliferation and matrix production [10].

Adhesion molecules are believed to participate in the pathogenesis of atherosclerosis [11]. These proteins regulate the interaction between the endothelium and the leukocytes, and an increase in their expression on the endothelial surface causes increased adhesion of leukocytes, particularly monocytes, which are well known as one of the first steps in the process leading to atheroma [11]. In particular, over-expression of intracellular adhesion molecule-1 (ICAM-1), vascular cell adhesion molecule-1 (VCAM-1), and E-selectin in endothelial cells in human atherosclerotic lesions has been reported [12]. The effects of high glucose concentrations on the expression of adhesion molecules in endothelial cells have been widely investigated. Increase of ICAM-1 has been reported in human aortic endothelial cells cultured in high glucose [13]; these data are consistent with findings indicating that high glucose is a potent promoter of leukocyte adhesion to endothelial cells under flow conditions, depending on upregulation of E-selectin, ICAM-1, and VCAM-1 [8].

The search for anti-inflammatory agents from natural herbal medicines has attracted considerable interest [14]. After screening several dozen commonly used herbs, we found that compounds from herbal medicines efficiently exhibited anti-inflammatory responses [12]. In a recent study, we reported that a new compound, emodin-6-*O*-β-D-glucoside (EG) from *Reynoutria japonica*, has anti-inflammatory and barrier protective effects in human endothelial cells and in mice [15]. However, no studies on high-glucose-induced inflammatory responses EG have been reported. Therefore, in the current study, we attempted to determine whether EG can suppress the vascular inflammatory process induced by HG in primary cultured human endothelial cells and in mice.

MATERIALS AND METHODS

Reagents

D-glucose, L-glucose, D-mannitol, Evans blue, 2-mercaptoethanol, and antibiotics (penicillin G and streptomycin) were purchased from Sigma (St. Louis, MO, USA). Fetal bovine serum (FBS) and Vybrant DiD were purchased from Invitrogen (Carlsbad, CA, USA). EG was organically synthesized (Supporting material).

Cell Culture

Primary human umbilical vein endothelial cells (HUVECs) were obtained from Cambrex Bio Science (Charles City, IA, USA) and maintained as described previously [16]. Briefly, cells were cultured to confluency at 37 °C and 5 % CO_2 in EBM-2 basal media supplemented with growth supplements (Cambrex Bio Science). THP-1 cells, a monocyte cell line, were maintained as previously described [17].

Animals and Husbandry

Male C57BL/6 mice (6–7 weeks old, weighting 18–20 g) purchased from Orient Bio Co. (Sungnam, KyungKiDo, Republic of Korea) were used in this study after a 12-day acclimatization period. Animals were housed five per polycarbonate cage under controlled temperature (20–25 °C) and humidity (40–45 %) and a 12:12 h light/dark cycle. Animals were supplied a normal rodent pellet diet and water *ad libitum* during acclimatization. All animals were treated in accordance with the Guidelines for the Care and Use of Laboratory Animals issued by Kyungpook National University.

Permeability Assay *In Vitro*

Endothelial cell permeability in response to increasing concentrations of EG was quantified by spectrophotometric measurement of the flux of Evans-blue-bound albumin across functional cell monolayers using a modified two-compartment chamber model. HUVECs were plated (5×10^4/well) in 3-μm pore size, 12-mm-diameter transwells for three days. Confluent monolayers were incubated with increasing concentrations of EG for 6 h, followed by incubation with indicated concentrations of high glucose for 24 h. Then, transwell inserts were washed with PBS (pH 7.4), followed by addition of 0.5 ml of Evans blue (0.67 mg/ml) diluted in growth medium containing 4 % BSA. Fresh growth medium was then added to the lower chamber, and the medium in the upper chamber was replaced with Evans blue/BSA. Ten minutes later, optical density was measured at 650 nm in the lower chamber.

Permeability Assays *In Vivo*

Mice were pretreated with intravenous administration of EG (4.5 or 9.0 μg/mouse), and after 6 h, 1 % Evans blue dye solution in normal saline was administered by intravenous injection in each mouse, immediately followed by an intravenous injection of high glucose (9 mg/kg).

Thirty minutes later, the mice were sacrificed and the peritoneal exudates were collected after being washed with 5 ml of normal saline and centrifuged at 200×*g* for 10 min. The absorbance of the supernatant was read at 650 nm. Vascular permeability was expressed in terms of dye (microgram per mouse), which leaked into the peritoneal cavity according to a standard curve of Evans blue dye, as previously described [18, 19].

Cell Viability Assay

Cells were grown in 96-well plates at a density of 5×10^3 cells/well for 24 h, washed with fresh medium, treated with indicated EG for 48 h, and washed, and 100 μl of MTT (1 mg/ml) was added, followed by incubation for 4 h. Finally, DMSO (150 μl) was added in order to solubilize the formazan salt, and the amount of formazan salt formed was determined by measurement of OD at 540 nm using a microplate reader (Tecan Austria GmbH, Austria). Data are expressed as the mean ± SD of at least three independent experiments.

Expression of Cell Adhesion Molecules (CAMs)

Expression of VCAM-1, ICAM-1, and E-selectin was determined by whole-cell ELISA. Briefly, HUVEC monolayers were treated with EG at the indicated concentrations for 6 h, followed by treatment with high glucose (25 mM) for 24 h, and fixed in 1 % paraformaldehyde. After washing three times, mouse anti-human monoclonal antibodies (VCAM-1, ICAM-1, and E-selectin, Temecula, CA, USA, 1:50 each) were added, and cells were incubated for 1 h (37 °C, 5 % CO_2). Cells were then washed, treated with peroxidase-conjugated anti-mouse IgG antibody (Sigma, St. Louis, MO, USA) for 1 h, washed three times, and then developed using *o*-phenylenediamine substrate (Sigma, St. Louis, MO, USA). All measurements were performed in triplicate wells.

Cell–Cell Adhesion Assay

Adherence of monocytes to endothelial cells was evaluated by fluorescent labeling of monocytes. Briefly, monocytes were labeled with 5 μM Vybrant DiD for 20 min at 37 °C in phenol red-free RPMI containing 5 % fetal bovine serum. Following two washings, cells (1.5×10^6/ml, 200 μl/well) were resuspended in adhesion medium (RPMI containing 2 % fetal bovine serum and 20 mM HEPES) and added to confluent monolayers of HUVECs in 96-well plates, which were treated for 6 h with EG or rutin followed by high glucose (25 mM for 24 h). Fluorescence of labeled cells was measured (total signal) using a fluorescence microplate reader (Tecan Austria GmbH, Austria). After incubation for 1 h at 37 °C, non-adherent cells were removed by washing four times with prewarmed RPMI, and the fluorescent signals of adherent cells were measured using previously described methods. The percentage of adherent monocytes was calculated using the formula: % adherence = (adherent signal/total signal) × 100 as described [20, 21].

RNA Preparation and Real-Time qRT-PCR

HUVECs were grown in six-well plates and incubated with EG for 6 h, followed by HMGB1 25 mM for 24 h. The High Pure RNA Isolation Kit from Roche Diagnostics was used for isolation of RNA from cell cultures, and RNA quality was tested by measuring the ratio 260/280 nm in a UV–spectrophotometer. For each sample, 0.5 μg of total RNA was reverse transcribed into cDNA using the Transcriptor First Strand cDNA Synthesis kit (Roche Diagnostics).

Real-time PCR analysis was performed using the LightCycler® 96 System (Roche Diagnostics, Mannheim, Germany) using FastStart Essential DNA Green Master (Roche Diagnostics) according to the manufacturer's instructions. GAPDH was used as an internal control. The relative quantification of mRNA expression was calculated as a ratio of the target gene to GAPDH. Specific sense and anti-sense primers used were as follows: MCP-1, sense: 5′-TGCAGAGGCTCGCGAGCTA-3′, anti-sense: 5′-CAGGTGGTCCATGGAATCCTGA-3′; IL-8, sense: 5′-ACTGAGAGTGATTGAGAGTGGAC-3′, anti-sense: 5′-AACCCTCTGCACCCAGTTTTC-3′; GAPDH, sense: 5′-GTCTTCACTACCATGGAGAAGG-3′, anti-sense: 5′-TCATGGATGACCTTGGCCAG-3′.

H_2O_2 Release Assay

Extracellular production of H_2O_2 was quantified using the Amplex Red Hydrogen Peroxide Assay Kit (Molecular Probes; Eugene, OR, USA) according to the manufacturer's recommendations. The cells were washed twice with ice-cold PBS and harvested by microcentrifugation and resuspended in a Krebs-Ringer phosphate (KRPG) solution; 100 μl of the reaction mixture (50 μM Amplex Red reagent containing 0.1 U/ml HRP in KRPG) was added to each microplate well and then prewarmed at 37 °C for 10 min. Then, the reaction was started by addition of resuspended cells in 20 μl of KRPG. Fluorescence readings became stable within 30 min of starting the reaction equipped for absorbance at 560 nm (Multiskan, Thermo Labsystems Inc,

Franklin, MA, USA). A reagent H_2O_2 standard curve was used for calculation of H_2O_2 concentration.

Preparation of Cytoplasmic and Nuclear Extracts

The cells were harvested rapidly by sedimentation, and nuclear and cytoplasmic extracts were prepared on ice, as previously described [22]. Cells were harvested and washed with 1 ml buffer A (10 mM HEPES, pH 7.9, 1.5 mM $MgCl_2$, 19 mM KCl) for 5 min at 600 g. The cells were resuspended in buffer A and then centrifuged at 600×*g* for 3 min, resuspended in 30 μl buffer B (20 mM HEPES, pH 7.9, 25 % glycerol, 0.42 M NaCl, 1.5 mM $MgCl_2$, 0.2 mM EDTA), rotated for 30 min at 4 °C, and then centrifuged at 13,000×*g* for 20 min. The supernatant was used as a nucleus extract. The nucleus and cytosolic extracts were then analyzed for protein content using Bradford assay.

Western Blotting

Total cell extracts were prepared by lysing the cells, and protein concentration was determined using Bradford assay methods. Equal amounts of protein were separated by SDS-PAGE (10 %) and electroblotted overnight onto an Immobilon membrane (Millipore, Billerica, MA, USA). The membranes were blocked for 1 h with 5 % low-fat milk-powder TBS (50 mM Tris–HCl, pH 7.5, 150 mM NaCl) containing 0.05 % Tween 20 and then incubated with either anti-VCAM-1, anti-ICAM-1, anti-E-selectin (1:500 Millipore, Billerica, MA, USA), or NF-κB p65 for 1.5 h at room temperature (1:1,000, Santa Cruz, CA, USA), followed by incubation with horseradish-peroxidase-conjugated secondary antibody and ECL-detection according to the manufacturer's instructions.

Immunofluorescence Staining

HUVECs were grown to confluence on glass cover slips coated with 0.05 % poly-L-lysine in complete media containing 10 % FBS and maintained for 48 h. Cells were then stimulated with high glucose (25 mM) for 1 h with or without prior treatment with EG (5 or 10 μM) for 2 h. After several washes with PBS, cells were fixed in 4 % formaldehyde in PBS (*v*/*v*) for 15 min at room temperature, and for immunostaining, cells were permeabilized in 0.05 % Triton X-100 in PBS for 15 min and blocked in blocking buffer (5 % BSA in PBS) overnight at 4 °C. Cells were incubated with primary rabbit monoclonal NF-κB p65 antibody, anti-rabbit alexa 488 overnight at 4 °C. Nuclei were counterstained with 4,6-diamidino-2-phenylindole dihydrochloride (DAPI). Cells were then visualized by confocal microscopy at a ×63 magnification (TCS-Sp5, Leica Microsystems, Germany).

Statistical Analysis

Results are expressed as mean ± standard error of mean (SEM) of at least three independent experiments. Statistical significance was determined using analysis of variance (ANOVA; SPSS, version 14.0, SPSS Science, Chicago, IL, USA), and *p*-values less than 0.05 ($p<0.05$) were considered significant.

RESULTS AND DISCUSSION

EG is found in *R. japonica*; we recently reported that EG has vascular barrier protective effects in high mobility group box 1 (HMGB1)-activated HUVECs and a cecal ligation and puncture (CLP) model of sepsis in mice [15]. In this study, the effects of EG (Supplementary Fig. 1) on HG-induced vascular inflammation were determined *in vitro* and *in vivo*.

Effects of EG on HG-Induced Disruption of the Endothelial Barrier Function of HUVECs and in Mice

Previous evidence has suggested that endothelial dysfunction and damage are early steps in the pathophysiology of vascular complications in diabetes mellitus [2, 23]. Hyperglycemia is the central initiating factor for all types of diabetic microvascular disease, and it may also be involved in the pathogenesis of macrovascular complications [1, 23]. Similarly, an increase in endothelial permeability has been implicated in early diabetic nephropathy [10, 24]. Therefore, we first investigated the effects of glucose on the albumin permeability of endothelial cells, as shown in Fig. 1a. Treatment with HG (25 and 50 mM) led to a rapid increase in endothelial cell permeability (Fig. 1a). This effect began from 12 h after incubation and reached its maximum at 24 h (Fig. 1b). A significant increase was observed at a glucose concentration of 10 mM. Concentrations above 50 mM did not further increase the glucose-induced permeability (data not shown). L-glucose and D-mannose (25 mM),

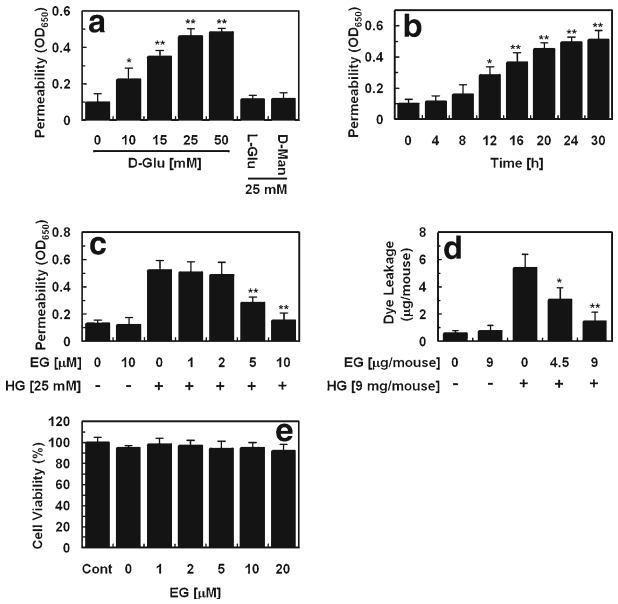

Fig. 1. Effects of EG on HG-mediated permeability *in vitro* and *in vivo*. **a** HUVECs were treated with D-glucose (0–50 mM), L-glucose (25 mM), and D-mannitol (25 mM) for 24 h, and permeability was monitored by measuring the flux of Evans-blue-dye-bound albumin across HUVECs. **b** HUVECs were treated with D-glucose (25 mM) for indicated time periods and permeability was monitored. **c** The effects of pretreatment with different concentrations of EG for 6 h on barrier disruptions caused by 25 mM HG for 24 h. **d** The effects of EG (i.v. injection) on HG-induced (9 mg/mouse, i.v.) vascular permeability in mice were determined by measuring the levels of Evans blue dye in peritoneal washings (expressed in microgram per mouse, $n=5$). **e** The effects of EG on cellular viability were determined using an MTT assay. Results are expressed as the mean ± SEM of at least three independent experiments. *$p<0.05$ and **$p<0.01$ *versus* 0 (**a**, **b**), HG alone (**c**, **d**).

which were used as an osmotic control, had no significant effect on endothelial cell permeability (Fig. 1a).

Next, we attempted to determine whether EG could alter HG-induced hyperpermeability. Treatment with 10 μM EG alone did not result in alteration of barrier integrity (Fig. 1c). As shown in Fig. 1c, treatment with EG resulted in a dose-dependent decrease in HG-mediated membrane disruption. To confirm this vascular barrier protective effect *in vivo*, HG-mediated vascular permeability in mice was assessed. As shown in Fig. 1d, treatment with EG resulted in markedly inhibited peritoneal leakage of dye induced by HG. Assuming that the average weight of a mouse was 20 g and the average blood volume was 2 ml, the amount of EG injected (4.5 or 9.0 μg per mouse) was equivalent to 5 or 10 μM in peripheral blood. To assess the cytotoxicity of EG, cell viability assays were performed in HUVECs treated with EG for 24 h. At concentrations up to 20 μM, EG did not affect cell viability (Fig. 1e). These findings demonstrate inhibition of HG-mediated endothelial disruption and maintenance of human endothelial cell barrier integrity by EG in mice treated with HG. Therefore, prevention of HG-induced release of HMGB1 by EG suggests the potential of EG in treatment of vascular inflammatory diseases.

Effects of EG on HG-Mediated Expression of CAMs and THP-1 Adhesion

One of the earliest events in the vascular inflammation process is adhesion of monocytes to the endothelium, which is followed by their infiltration and differentiation into macrophages [25]. This key step is mediated by an interaction between monocytes and molecules expressed on the surface of endothelial cells [25]. These CAMs primarily mediated the adhesion of monocytes specifically found in atherosclerosis lesions of the vascular endothelium [25]. Therefore, we determined the effects of HG on expression of CAMs and adhesion of monocytes to HUVECs in response to HG. The responses according to the concentration of HG in the expression of CAMs, such as VCAM-1, ICAM-1, and E-selectin, were determined by cell ELISA and Western blotting. Exposure of the primary cultured HUVECs to HG resulted in significantly increased expression of VCAM-1, ICAM-1, and E-selectin after incubation with 25 mM D-glucose; the maximum inhibitory effect of EG was observed at 5 μM (Fig. 2a, b). In addition, in order to explore the effect of EG on endothelial cell–leukocyte interaction, we examined adhesion of THP-1 cells to high-glucose-activated HUVECs. Control HUVECs showed minimal binding to THP-1 cells; however, adhesion showed a marked increase upon treatment with HG. Pretreatment with EG (5–10 μM) resulted in a decrease in the number of THP-1 cells adhering to HG-induced HUVECs (Fig. 2c, d). Thus, EG could be used as a therapeutic drug candidate for diabetic vascular inflammation targeting CAM expression in prevention of atherosclerotic lesions.

MCP-1 and IL-8 are the chemokines most strongly implicated in the atherogenesis process [26]. MCP-1 is a key mediator of monocyte trafficking, and IL-8 is chemotactic for neutrophils [26]. Thus, we measured the effect of EG on HG-induced MCP-1 and IL-8 mRNA level using real-time qRT-PCR. As shown in Fig. 3, HG

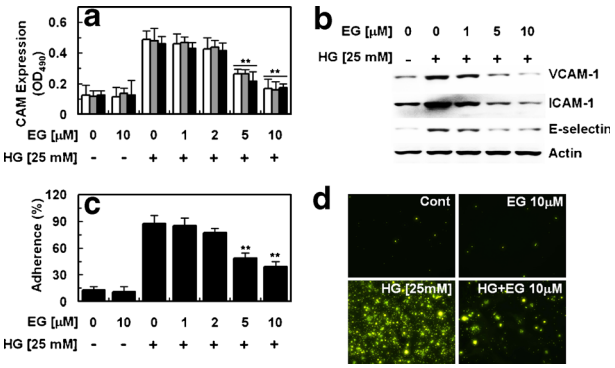

Fig. 2. Effects of EG on HMGB1-mediated pro-inflammatory responses. **a**, **b** HG-induced (25 mM, for 24 h) expression of cell adhesion molecules on HUVECs was determined after treatment of cells with the indicated concentrations of EG for 6 h. VCAM-1 (*white bar*), ICAM-1 (*gray bar*), and E-selectin (*black bar*) were detected by **a** ELISA and **b** Western blotting analysis. **c**, **d** HG-induced (25 mM, for 24 h) adherence of monocytes to HUVEC monolayers was assessed after pretreatment of cells with EG for 6 h. The amounts of adherent THP-1 cells were monitored by **c** cell–cell adhesion assay and **d** fluorescence microscopy. Data are expressed as the mean ± SEM of three independent experiments. $^{**}p<0.01$ *versus* HG alone.

induced an increase in expression levels of MCP-1 (up to 3.8-fold) and IL-8 (up to 4.6-fold) mRNA, and pretreatment with EG resulted in decreased expression levels of HG-induced MCP-1 and IL-8 mRNA. These results suggested that EG may be useful in the prevention of the vascular inflammatory process.

Effect of EG on HG-Induced Oxidative Stress

Inflammatory responses have been mechanistically linked to production of reactive oxygen species (ROS) [27]. Previous observations have indicated that hyperglycemia triggers generation of free radicals, and oxidant

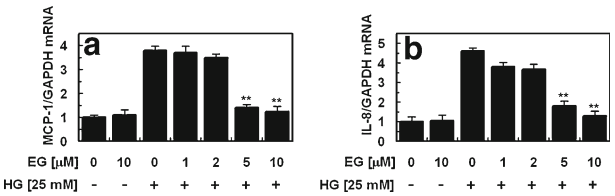

Fig. 3. Effects of EG on HG-induced expression of MCP-1 and IL-8 mRNA in HUVECs. Cells were pretreated with indicated concentrations of EG for 6 h and then incubated with HG (25 mM) for 48 h. mRNA was extracted, and real-time qRT-PCR analysis was performed using specific primer for MCP-1, IL-8, and GAPDH, as described in the "MATERIALS AND METHODS" section. Data are expressed as the mean ± SEM of three independent experiments. $^{**}p<0.01$ *versus* HG alone.

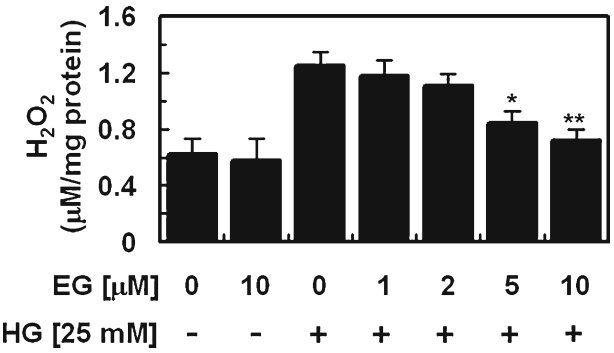

Fig. 4. Effects of EG on HG-induced ROS formation. Cells were pretreated with EG (0–10 μM) for 6 h and then stimulated with HG for 1 h; H_2O_2 assay was then performed as described in the "MATERIALS AND METHODS" section. Data are expressed as the mean ± SEM of three independent experiments. $^{*}p<0.05$ and $^{**}p<0.01$ *versus* HG alone.

stress in various cell types and ROS are considered to be important mediators of several biologic responses, including cell proliferation and extracellular matrix deposition [28, 29]. Therefore, to examine the protective effect of EG in HG-induced oxidative stress, we measured the effect of HG on cellular H_2O_2 concentration. The H_2O_2

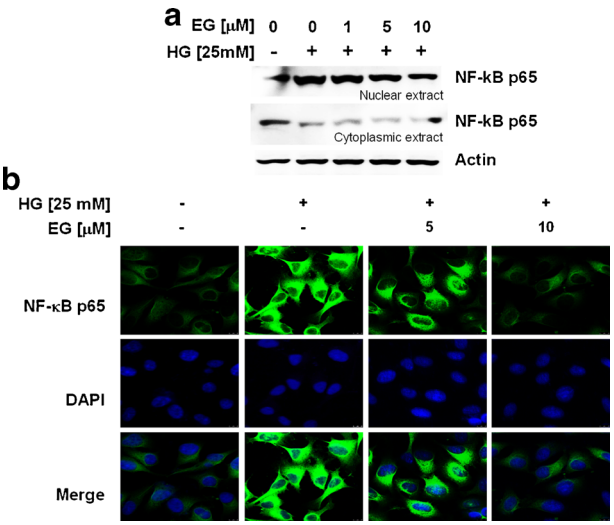

Fig. 5. Effects of EG on HG-induced activation of NF-κB. **a** Cells were pretreated with EG (0–10 μM) for 6 h and then stimulated with HG for 1 h. **b** NF-κB p65 was visualized using rabbit anti-p65 monoclonal antibody (1:100), which only recognized NF-κB p65. Goat anti-rabbit antibody (1:100) conjugated to FITC was performed. The subcellular localization of NF-κB p65 was examined by immunofluorescence staining and visualized under an immunofluorescence microscope. The images are representative of results from three independent experiments.

level showed a statistically significant increase after incubation for 10 min with 25 mM glucose, and a maximal increase was observed at 1 h (data not shown). Thus, we chose to determine cellular ROS at 1 h after glucose treatment in subsequent experiments. As shown in Fig. 4, pretreatment with 5 and 10 μM EG resulted in significantly inhibited HG-induced H_2O_2 level. In addition, EG itself did not induce oxidative stress (Fig. 4), which suggested the importance of high-glucose-induced oxidative stress from HUVECs in determining the character of diabetic complication as well as vascular inflammation. In addition, pretreatment with EG resulted in significantly inhibited high-glucose-induced ROS formation, suggesting a role of antioxidant activity.

Effect of EG on HG-Induced Activation of NF-κB

Activation of transcription factors such as NF-κB is known to affect CAMs and to induce a coordinated upregulation of other pro-inflammatory cytokines and chemoattractants, which possibly provides the molecular link between cell redox state and endothelial cell dysfunction [30]. In addition, ROS has been shown to activate various transcription factors, including NF-κB in cultured endothelial cells [31]. First, we measured HG-induced translocation of NF-κB from cytosol to nucleus. In Western blotting analysis for determination of NF-κB p65 protein level, the active subunit of the NF-κB complex, an increase in the level of the p65 protein was observed in the nuclear extracts of HUVECs treated with HG, and the cytosolic extracts exhibited an appreciable loss of p65 protein content (Fig. 5a). In addition, pretreatment with EG resulted in inhibition of the HG-induced increase of p65 NF-κB expression levels (Fig. 5a). To confirm consistency with the result of Western blotting, immunocytochemistry was performed using p65 NF-κB and fluorescein isothiocyanate (FITC)-conjugated antibody. As a result, HG induced an increase in expression of p65 NF-κB in the nucleus, whereas normal condition did not. In addition, treatment with 5 and 10 μM EG resulted in a decrease in HG-induced expression of p65 NF-κB in the nucleus. These results were consistent with those of Western blotting (Fig. 5b), demonstrating that HG-induced activation of NF-κB was inhibited by EG, indicating that EG has some inhibitory effect on the NF-κB pathways specific to HG-induced adhesion molecules in HUVECs.

In summary, our results demonstrate that treatment with EG resulted in blockade of HG-induced vascular inflammation via inhibition of ROS and NF-κB in primary human endothelial cells. These results suggest that EG has significant therapeutic benefits against diabetic complications and atherosclerosis by attenuating HG-induced generation of H_2O_2, increased activation of NF-κB, upregulation of adhesion molecules, monocyte–endothelial adhesion, and disruption of the endothelial barrier function. Our findings indicate that EG can be regarded as a candidate for use in treatment of diabetic vascular inflammatory diseases.

ACKNOWLEDGMENTS

This study was supported by the National Research Foundation of Korea (NRF) funded by the Korean Government [MSIP] (Grant No. 2012–000940).

Conflict of Interest. The authors declare no conflicts of interest.

REFERENCES

1. Kannel, W.B., and D.L. McGee. 1979. Diabetes and cardiovascular disease. The Framingham study. *JAMA* 241: 2035–2038.
2. Kannel, W.B., and D.L. McGee. 1979. Diabetes and glucose tolerance as risk factors for cardiovascular disease: the Framingham study. *Diabetes Care* 2: 120–126.
3. Chistiakov, D.A. 2011. Diabetic retinopathy: pathogenic mechanisms and current treatments. *Diabetes Metabolic Syndrome* 5: 165–172.
4. Gerrity, R.G. 1981. The role of the monocyte in atherogenesis: I. Transition of blood-borne monocytes into foam cells in fatty lesions. *American Journal of Pathology* 103: 181–190.
5. Wardle, E.N. 1994. Vascular permeability in diabetics and implications for therapy. *Diabetes Research and Clinical Practice* 23: 135–139.
6. Esposito, C., G. Fasoli, A.R. Plati, *et al*. 2001. Long-term exposure to high glucose up-regulates VCAM-induced endothelial cell adhesiveness to PBMC. *Kidney International* 59: 1842–1849.
7. Hamuro, M., J. Polan, M. Natarajan, and S. Mohan. 2002. High glucose induced nuclear factor kappa B mediated inhibition of endothelial cell migration. *Atherosclerosis* 162: 277–287.
8. Morigi, M., S. Angioletti, B. Imberti, *et al*. 1998. Leukocyte–endothelial interaction is augmented by high glucose concentrations and hyperglycemia in a NF-κB-dependent fashion. *Journal of Clinical Investigation* 101: 1905–1915.
9. Tooke, J.E. 1995. Microvascular function in human diabetes. A physiological perspective. *Diabetes* 44: 721–726.
10. Nannipieri, M., L. Rizzo, A. Rapuano, A. Pilo, G. Penno, and R. Navalesi. 1995. Increased transcapillary escape rate of albumin in microalbuminuric type II diabetic patients. *Diabetes Care* 18: 1–9.
11. Lopes-Virella, M.F., and G. Virella. 1992. Immune mechanisms of atherosclerosis in diabetes mellitus. *Diabetes* 41(Suppl 2): 86–91.
12. Bae, J.S. 2012. Role of high mobility group box 1 in inflammatory disease: focus on sepsis. *Archives of Pharmacal Research* 35: 1511–1523.
13. Kado, S., T. Wakatsuki, M. Yamamoto, and N. Nagata. 2001. Expression of intercellular adhesion molecule-1 induced by high

glucose concentrations in human aortic endothelial cells. *Life Sciences* 68: 727–737.
14. Aggarwal, B.B., H. Ichikawa, P. Garodia, *et al*. 2006. From traditional Ayurvedic medicine to modern medicine: identification of therapeutic targets for suppression of inflammation and cancer. *Expert Opinion on Therapeutic Targets* 10: 87–118.
15. Lee, W., S.K. Ku, T.H. Kim, and J.S. Bae. 2013. Emodin-6-*O*-beta-D-glucoside inhibits HMGB1-induced inflammatory responses *in vitro* and *in vivo*. *Food and Chemical Toxicology* 52: 97–104.
16. Qureshi, S.H., C. Manithody, J.S. Bae, L. Yang, and A.R. Rezaie. 2008. Autolysis loop restricts the specificity of activated protein C: analysis by FRET and functional assays. *Biophysical Chemistry* 134: 239–245.
17. Kim, T.H., and J.S. Bae. 2010. *Ecklonia cava* extracts inhibit lipopolysaccharide induced inflammatory responses in human endothelial cells. *Food and Chemical Toxicology* 48: 1682–1687.
18. Bae, J.S., W. Lee, and A.R. Rezaie. 2012. Polyphosphate elicits proinflammatory responses that are counteracted by activated protein C in both cellular and animal models. *Journal of Thrombosis and Haemostasis*.
19. Lee, J.D., J.E. Huh, G. Jeon, *et al*. 2009. Flavonol-rich RVHxR from *Rhus verniciflua* stokes and its major compound fisetin inhibits inflammation-related cytokines and angiogenic factor in rheumatoid arthritic fibroblast-like synovial cells and *in vivo* models. *International Immunopharmacology* 9: 268–276.
20. Akeson, A.L., and C.W. Woods. 1993. A fluorometric assay for the quantitation of cell adherence to endothelial cells. *Journal of Immunological Methods* 163: 181–185.
21. Kim, I., S.O. Moon, S.H. Kim, H.J. Kim, Y.S. Koh, and G.Y. Koh. 2001. Vascular endothelial growth factor expression of intercellular adhesion molecule 1 (ICAM-1), vascular cell adhesion molecule 1 (VCAM-1), and E-selectin through nuclear factor-kappa B activation in endothelial cells. *Journal of Biological Chemistry* 276: 7614–7620.
22. Mackman, N., K. Brand, and T.S. Edgington. 1991. Lipopolysaccharide-mediated transcriptional activation of the human tissue factor gene in THP-1 monocytic cells requires both activator protein 1 and nuclear factor kappa B binding sites. *Journal of Experimental Medicine* 174: 1517–1526.
23. Laakso, M. 1999. Hyperglycemia and cardiovascular disease in type 2 diabetes. *Diabetes* 48: 937–942.
24. Sander, B., M. Larsen, C. Engler, H. Lund-Andersen, and H.H. Parving. 1994. Early changes in diabetic retinopathy: capillary loss and blood–retina barrier permeability in relation to metabolic control. *Acta Ophthalmologica* 72: 553–559.
25. Hansson, G.K., and P. Libby. 2006. The immune response in atherosclerosis: a double-edged sword. *Nature Reviews Immunology* 6: 508–519.
26. Boisvert, W.A. 2004. Modulation of atherogenesis by chemokines. *Trends in Cardiovascular Medicine* 14: 161–165.
27. Inoguchi, T., P. Li, F. Umeda, *et al*. 2000. High glucose level and free fatty acid stimulate reactive oxygen species production through protein kinase C-dependent activation of NAD(P)H oxidase in cultured vascular cells. *Diabetes* 49: 1939–1945.
28. Dunlop, M. 2000. Aldose reductase and the role of the polyol pathway in diabetic nephropathy. *Kidney International. Supplement* 77: S3–S12.
29. Han, H.J., Y.J. Lee, S.H. Park, J.H. Lee, and M. Taub. 2005. High glucose-induced oxidative stress inhibits Na+/glucose cotransporter activity in renal proximal tubule cells. *American Journal of Physiology. Renal Physiology* 288: F988–F996.
30. Rimbach, G., G. Valacchi, R. Canali, and F. Virgili. 2000. Macrophages stimulated with IFN-gamma activate NF-kappa B and induce MCP-1 gene expression in primary human endothelial cells. *Molecular Cell Biology Research Communications* 3: 238–242.
31. Uemura, S., H. Matsushita, W. Li, *et al*. 2001. Diabetes mellitus enhances vascular matrix metalloproteinase activity: role of oxidative stress. *Circulation Research* 88: 1291–1298.